

Meaning in Architecture, now

Original

Meaning in Architecture, now / Deregibus, Carlo; Alison, Aurorarosa. - In: PHILOSOPHY KITCHEN. - ISSN 2385-1945. - ELETTRONICO. - 21:(2024), pp. 1-258.

Availability:

This version is available at: 11583/2995796 since: 2025-01-23T13:39:45Z

Publisher:

Università degli Studi di Torino

Published

DOI:

Terms of use:

This article is made available under terms and conditions as specified in the corresponding bibliographic description in the repository

Publisher copyright

(Article begins on next page)

Modulation of sonochemical reactions by cavitation driven thermal degradation of aqueous salts solutions

Received: 15 July 2025

Accepted: 20 February 2026

Cite this article as: Troia, A., Gallone, M., Vighetto, V. *et al.* Modulation of sonochemical reactions by cavitation driven thermal degradation of aqueous salts solutions. *Commun Chem* (2026). <https://doi.org/10.1038/s42004-026-01961-4>

A. Troia, M. Gallone, V. Vighetto, F. Pellegrino, S. Hernández, V. Cauda & V. Maurino

We are providing an unedited version of this manuscript to give early access to its findings. Before final publication, the manuscript will undergo further editing. Please note there may be errors present which affect the content, and all legal disclaimers apply.

If this paper is publishing under a Transparent Peer Review model then Peer Review reports will publish with the final article.

Modulation of sonochemical reactions by cavitation driven thermal degradation of aqueous salts solutions

Troia^{1*}, *M. Gallone*², *V. Vighetto*², *F. Pellegrino*³, *S. Hernández*², *V. Cauda*², *V. Maurino*³

1 Ultrasounds & Chemistry Lab, Advanced Metrology for Quality of Life, Istituto Nazionale di Ricerca Metrologica (I.N.Ri.M.), Strada delle Cacce 91, Turin, 10135, Italy

2 Department of Applied Science and Technology, Politecnico di Torino, Corso Duca degli Abruzzi 24, Turin, 10129, Italy

3 Department of Chemistry, University of Torino, Via Giuria 7 10125, Torino, Italy

Strategies for controlling or increasing the yield of radical reactions generated by ultrasonic cavitation in aqueous media have been the object of research for many years. Past studies have focused on the role of organic solvents in increasing Reactive Oxygen Species (ROS) formation or have investigated the effect of ultrasound on accelerating the OH radicals generation from Fenton reactive. More recently, piezoelectric micro-nanoparticles have shown a synergistic effect in activating specific reactions and increasing radicals production from ultrasound. Here we report the generation of ROS together with H₂ evolution or increase of oxidizing species during ultrasonic treatments of homogeneous concentrated aqueous solutions of simple salts as acidic phosphates, potassium sodium tartrate and alkaline nitrates. An increase in organic dye degradation efficiency, and the increase of reducing or oxidizing species compared with pure water has been found. The activation mechanism revealed a new, unexpected, approach to enhance the efficiency of sono-catalysed reactions in aqueous media for environmental or energy applications.

Keywords: Cavitation, ROS scavenging, hydrogen, homogeneous sonochemistry

Highlights

- *Activation of new son-catalysed chemical reactions in homogenous solutions of concentrated salts*
- *Increase of hydrogen production or oxidizing species as function of salt used*
- *Increase of degradation efficiency using simple cheap salts*
- *Thermal degradation of salt molecules by liquid droplets injection within collapsing bubbles*

Introduction

Acoustic cavitation refers to the nucleation, growth, and violent implosion of microbubbles generated by high-intensity ultrasound in liquid media [1]. Under these conditions bubbles behave as local hot spot in which extremely high temperature ($> 10.000 \text{ }^\circ\text{K}$) and pressure ($> 10\text{MPa}$) are reached [2] leading light emission (Sonoluminescence, SL) by the formation of short living microplasma, [3], [4] which cause the breakage and ionization of gas or vapour molecules, present inside the bubbles during the collapse. In case of aqueous solutions, several radical oxidizing species (ROS) are produced, arising from the sonochemical splitting of water molecules and the formation of HO^\cdot and H^\cdot species [5] [6]. Acoustic streaming promote physical effects inducing high shear stress near the bubbles, with the formation of microjets, microstreaming, and shock waves, which can cause the exposure of dispersed solid particles or the injection of liquid microdroplets to these extreme conditions [7]. These physical and chemical effects form the foundation of sonochemistry, which involves the application of ultrasound to

activate or accelerate chemical and physical processes [8], [9]. The efficiency of a sonochemical process depends on several parameters like liquid nature, temperature, or in other terms, its vapour pressure, gas dissolved, ultrasonic frequency, and acoustic pressure, or in other words, ultrasound power. However, the current lack of control over this phenomenon has limited its use in energy and environmental applications due to the low efficiency of sonochemical treatments [8,9,10]. In general, physical or mechanical effects as shear stress forces, shock waves, are dominant at low frequencies (20-80 kHz) [13] while at high frequencies (500kHz-1MHz) chemical effects as increase of hydroxyl radicals yields are usually reported [14]. Historically, numerous studies have aimed to increase the yield of sonochemical processes by scavenging radicals produced in the bubbles and releasing more efficient reactive species in the bulk solution. Recent models have focused on optimizing acoustic parameters (US frequency and power) to obtain efficient water splitting and hydrogen production [15]. Several investigations have reported the use of organic volatile solvents, such as alcohols or glycol, as radical scavengers in aqueous solutions, since they accumulate in the bubbles, react with OH radicals, and increase ROS release in the bulk, thereby forming longer-lived radical species [16]. However, as the solvent concentration increases, the accumulation of these molecules reduces the energy of bubbles collapse, as a

consequence the amount of radicals decreases and the scavenging effect becomes negligible [17,18].

Recently, several studies have revealed the possibility to increase ROS formation or steer it toward the generation of a single product (H_2 or H_2O_2 , for example) using ultrasounds [19-24]. It has been largely reported that micro or nano-semiconductors or piezoelectric particles could enhance the efficiency of ultrasonic processes for several applications in environment, energetic, and biomedical fields [25-36]. However, the synergistic effects of piezocatalytic processes are still unclear as has also emerged in many recent works [37-43]. So far, all the studies involving mechanically driven catalysis (piezocatalysis, flexocatalysis, tribocatalysis, and sonocatalysis) [38] have mainly focused on heterogeneous aqueous systems. In this context investigations in the homogeneous phase are lacking, probably due by low selectivity of aqueous radical products and recombination undesired side reactions that limit the efficiency of the process. To the best of our knowledge, studies on sono-catalysed reactions in aqueous solutions of a piezoelectric salts have not been reported. For this reason, we investigated initially the effect of ultrasound on aqueous concentrated solutions of straightforward piezoelectric salts, to examine the formation of ROS or other reactive species, that lastly have revealed the activation of unexpected scavenging mechanisms, not related to their

piezoelectric properties, never reported before. We observed an increase of the selectivity on the production of reducing or oxidising and hydroxyl radicals species as function of different salts. We found evidences that exposure of salt molecules to the high transient temperatures of collapsing bubbles allows to activate new radicals pathway that are able to optimize the yield and nature of sonochemical products. Here we report a series of experimental investigations which shows as this mechanism may affects aqueous radical reactions both inside the bubbles, in the vapour phase, and the surrounding shell in the liquid phase.

Results and discussions

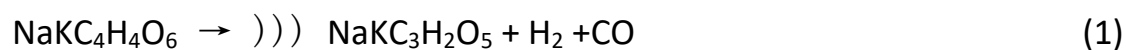
We investigated ultrasonic irradiation at both low frequency (20kHz) and high frequency (858 kHz) of saturated aqueous solutions of different piezoelectric salts as Potassium Sodium tartrate ($\text{KNaC}_4\text{H}_4\text{O}_6 \cdot 4\text{H}_2\text{O}$) and Dihydrogen Ammonium Phosphate ($\text{NH}_4\text{H}_2\text{PO}_4$) [44,45] and ferroelectric salts as Dihydrogen Potassium Phosphate KH_2PO_4 and Potassium Nitrate (KNO_3) [46,47] using sonochemical apparatus of Fig. S1, S2, S3 of S.I..

As quantitative measurements of OH^\bullet produced by ultrasound are still a matter of debate [48,49] we used spin trapping and photoluminescence probe measurements, together with gas chromatography, KI dosimetry, sonoluminescence spectra, and dyes degradation efficiency of Methylene Blue (MB), Methyl Orange (MO), and Bromophenol Blue (BB), for characterizing these solutions with respect to ultrasonic treatment in pure water.

Increase of reducing species

In particular, low-frequency ultrasonic treatment of a concentrated (30% in weight) Potassium Sodium tartrate (PST) solution causes an increase in reducing species, which was initially observed by reduction reaction of MB, rather than effective degradation (see S.I. Figure S8 captions details*) [50]. The increase in reducing species was successively confirmed by redox potential measurements of the solution: a decrease of 30-40% with respect to the initial potential value of the solution has been observed, after 1 h of ultrasonic treatment at 20 kHz. A further confirmation has been obtained using Resazurin (see Figure 1a), a dye probe [51], which changes its colour in the presence of reducing species. However, no OH^\bullet has been detected using the 5,5-dimethyl-1-pyrroline-*N*-oxide (DMPO) probe in EPR measurements or using Terephthalic acid (TA) in photoluminescence

investigations. To quantify the formation of reducing species, μ -GC measurements have been performed on sealed sonoreactors (figures S4 and S5 in S.I. and Material and method for details). It should be noted that after 15 minutes of sonication at 20 kHz (Figure 1b), a remarkable increase of H_2 as gas reaction's products with respect to sonication of pure water has been detected. Despite the low energy efficiency of this process, normalizing over time, 10 mmol/h of H_2 could be produced which is a remarkable value comparing to most of the data on hydrogen production using only ultrasound, as reported in [52,53] (see table in figure S8 of S.I.). At 858 kHz, an increase of Hydrogen production is still visible but the amount is similar to that produced at low frequency in water. These μ -GC measurements revealed also the formation of CO (figure 1C, red lines) suggests a sort of tartrate dehydrogenase reductive decarboxylation of PST activated by hot collapsing bubbles [54]. As reported in thermogravimetric (TG) analysis of the thermal decomposition of PST [55] the following reaction (1), in which))) symbol represent the action of ultrasonic waves, may occur.

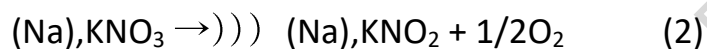


Increase of oxidizing species

Ultrasonic irradiation of concentrated solutions of KNO_3 provided further insight on this salt's activation mechanism. As no OH^\bullet have been detected from sonication of KNO_3 solutions both at 20 and 858 kHz using DMPO or TA probe, we have considered the well-known thermal degradation of this salt, which decomposes to O_2 and KNO_2 [56] and then investigated the formation of oxidizing species by different techniques: redox potential measurement, oxygen dissolved, u-GC and KI dosimetry method. As the first three methods didn't allow to establish the formation of oxidizing species we exploited the oxidation of Iodine to I_2 [57,58] to quantify the formation of oxidizing species in aqueous solutions, which can be easily detected with UV-vis absorbance spectroscopy of I_3^- complex [59].

We exposed a 0.1 M solution of KI to ultrasound using the set-up of Figure S1 and S3 in the S.I. . Then ultrasonic treatment was repeated by adding KNO_3 to this solution. Since UV-vis absorption of KNO_3 overlaps the region of I_3^- complex around 350 nm (see Figure S6 of S.I.), starch (0.1% in weight) was added to the solutions in order to evaluate the absorption of I_2 -starch complex around 500 nm. On the figure 2A and 2B it can be seen as the solutions treated with KNO_3 are more violet/dark with respect to one containing KI only and UV-vis measurements confirmed this increment both at 20 and 858 kHz. Ultrasonic irradiation activates thermal decomposition of KNO_3 forming O_2 that could scavenge H^\bullet arising from water

sonolysis. Then hydroperoxyl radical (HO_2^\bullet) can react, as proposed in following scheme (reaction 2-5) and thus increasing the release of oxidizing species into the bulk forming H_2O_2 reactions. Formation of NO_3^\bullet or different radical are also possible [60] but difficult to distinguish in this high ionic strength media. Finally, to confirm the thermal decomposition mechanism of nitrates we conducted similar experiment using a 30% solution of NaNO_3 instead of KNO_3 and similar effect were observed as can be noted from the figure 2C.



Increase of OH Radicals

The experiments with concentrated solutions of $\text{NH}_4\text{H}_2\text{PO}_4$ (ADP) and KH_2PO_4 (KDP) revealed a more complex mechanism, which involves the scavenging of aqueous OH^\bullet by acidic phosphates activated by cavitation bubbles.

As the results obtained with PST and KNO_3 , indicate that salt's thermal decomposition would be seem the key of these sono-catalysed mechanism, we included another acidic phosphate, NaH_2PO_4 (NaDP), which isn't

piezo/ferroelectric. With these salts we observed an increase of dyes degradation efficiency for Methylene Blue (MB), Methyl Orange (MO) and Bromophenol blue (BB), with respect to the use of pure water, both at low and at high frequency. Figure 3 shows the increase of MB degradation efficiency with the 20% solutions of these salts with respect to pure water (Figure 3A), and as a function of acidic phosphates concentration (Figure 3B). Figure 4 shows the degradation of MO as function of different phosphates (4A), UV-vis spectra of MO after treatment at 858 kHz in a 20% solution of ADP (Figure 4B) and the UV-vis spectra of Bromophenol Blue after treatment at 858 kHz in a 30% solution of ADP (Figure 4C). In order to evaluate the efficiency of salt activated degradation a common piezoelectric material has been also tested. Piezocatalytic degradation of MB and MO with commercial ZnO nanoparticles are shown in Fig. 3C and 4B compared with degradation efficiency of ADP and NaDP respectively. After ultrasonic treatment at 20 kHz for 30 min MB degradation resulted more efficient using 30% solution of ADP than ZnO nanoparticles (0.2% in weight) Fig. 3C red curve, while at 858 kHz NaDP resulted more efficient for MO degradation after 90 min of treatment respect ZnO, Fig. 4B black curve .

However, no OH^\bullet have been detected from EPR measurements, (see Figure S7 of the S.I.). On the contrary a variation of OH^\bullet radicals have been observed with

photoluminescence probe (TA) measurements. TA reacts with OH^\cdot forming a TA-OH luminescing molecule and its quantification measurements have been performed as a function of different salts, their concentration, and the ultrasonic frequency. We have carried out several experiments, both at 20 kHz and 858 kHz. Examples of photoluminescence (PL) spectra of TA after sonication at 20 kHz in pure water and solutions of KH_2PO_4 , $\text{NH}_4\text{H}_2\text{PO}_4$ and NaH_2PO_4 are reported in Figure 5A. Figure 5B shows the total PL signals quantification as function of different salt concentration.

In this case, it is worth noting that the PL intensity increases with respect to pure water when using a 10% solution of KDP and NaDP, while it decreases in the presence of ADP or when a higher salt concentration is used (Figure 5B). The experiments at 858 kHz show a similar trend, but with an interesting difference, as the PL intensity increases for the pure water using 10% solution of KDP, NaDP and ADP (Figure 5C). Then the PL signal drops to the value of the water sample as the salt concentration increases, except for the ADP solution, for which a decrease is observed (Figure 5D).

It's commonly accepted that TA underestimates the amount of OH^\cdot , since its low solubility prevents the accumulation inside the bubbles and can react only with

radicals released into the bulk [61]. Since we observed an increase in dye degradation as a function of salt concentration, it appeared evident that these anomalous trends in OH^\bullet quantification, dependent on salt concentration, type of cation, and ultrasonic frequency, revealed as further radical reactions may occur.

As for the case of PST and KNO_3 we considered the thermal decomposition reactions of these salts. Acidic phosphates, such as KH_2PO_4 , $\text{NH}_4\text{H}_2\text{PO}_4$, NaH_2PO_4 , are used as flame extinguishers [62] since they act as scavengers of reactive radical species produced by flames, suppressing chain reactions that lead to fire propagation and explosion [63,64]. Our results indicate a similar scenario, considering collapsing bubbles as “transient hot flames” suppressed by salts molecules. Salts inhibition mechanism involves both energy absorption by salt thermal decomposition and chemical scavenging by HOPO and HOPO_2 species with OH^\bullet and H^\bullet . Several reaction mechanisms have been proposed [65,66] and, for more clarity, a list of possible involved reactions is reported in table 1. As it can be seen from the table 1, scavenging reactions by phosphates could lead to many reactive radicals [67-75] that could contribute to dyes degradation.

Formation of radical species from acoustic cavitation can also be detected from the emission spectra of the sonoluminescence (SL) phenomenon. Since PO^\bullet emission

has been observed from sonoluminescence in H_3PO_4 [76], we performed multibubbles sonoluminescence experiments (see SI for experimental details) in aqueous 10% solutions of KDP, ADP, and NaDP compared to SL in H_2O and H_3PO_4 (85%) as a reference. Although the OH^\bullet and PO^\bullet radical emissions overlap in 280-350 nm region [77], qualitative results on different emission contributions in this region as a function of different salts have been carried out. In Figure 6 the emission spectra from different liquids and solutions are shown. In case of H_2O and H_3PO_4 the spectra confirm a series of results previously reported in the literature, such as the OH^\bullet emission in water at 310 nm (blue curve) or the CN emission at 385 nm, and PO emission at 340 nm in H_3PO_4 (black curve) [78]. SL spectra in KDP, NaDP solutions show the respective emission from alkali atoms (around 588-590 nm for Na^* and 770-772 nm for K^*) while a more intense contribution in the region between 280-350 nm have been observed in ADP solution, which may indicate the formation of PO^\bullet when using this salt. This qualitative information cannot be correlated to quantitative PL measurements, as the experimental conditions were different; however, sonoluminescence spectra support the formation of different radical species in the presence of acidic phosphates.

The results reported so far demonstrate, for the first time to the best of our knowledge, that the thermal decomposition of these salts, activated by hot

transient collapsing bubbles generated by ultrasound, can modify the yield of products in sono-catalyzed reactions under homogeneous conditions. The different results as a function of frequency highlighted how this mechanism can occur both within the bubbles and at the liquid-gas interface, as recently proposed [79]. In the case in which the salt generates a reducing specie, as for PST, a higher efficiency was observed at low frequency since it is known that at 20 kHz the amount of salt injected into collapsing bubbles as small droplets is higher [80]. In the presence of KNO_3 an increase in oxidizing species was observed at both frequencies. Previously the increment of H_2O_2 from sonication of aqueous solution of HNO_3 , NaNO_3 , and $\text{N}_2\text{H}_5\text{NO}_3$ have been reported [81,82] but a chemical catalysed reaction for the generation of NO_3^\bullet and its reaction with OH^\bullet was exploited in that case. In our experiments, the increase in oxidizing products arises from the thermal decomposition of KNO_3 or NaNO_3 by liquid droplet injection or salt exposure to a faintly warm liquid shell interface. As scavenging of H^\bullet radical and hydroperoxyl radical formation are strongly favoured in the liquid phase [68], this mechanism would lead to an increase in oxidizing species, since it also reduces the recombination rate of aqueous radicals.

The results obtained with acid phosphates also highlighted how this scavenging mechanism is influenced by ultrasound frequency, salt concentration and the

relative cations. At low frequency (figure 5A and 5B) the increase of PL intensity in 10 % solutions indicates a more efficient release of OH^\bullet in the bulk by scavenging from HOPO_2 , HOPO and relative radical mechanisms (5,6,7,9,10,11,13,14) of table 1, probably occurring at liquid-gas interface [68]. As the salt concentration increases, a major amount of phosphates molecules enter in the bubbles, lowering the release of OH^\bullet in the bulk because of other phosphates radical are formed. In case of $\text{NH}_4\text{H}_2\text{PO}_4$ this mechanism is enhanced by the reactions (3,4) of table 1 as NH_3 could form in the gas phase contributing to reduce OH^\bullet release [63,64,65]. This hypothesis is also supported by the results at high frequency: as a lower amount of liquid is injected into the bubbles at 858 kHz, then the formation of NH_3 is much lower. As a consequence, in 10% solutions the photoluminescence (PL) variations with respect to water for ADP follow a similar trend to KDP and NaDP, while in 20% solutions the PL signal decreases as more NH_3 could form in the gas phase. In flames suppression mechanisms the physical energetic adsorption from thermal degradation process and from chemical radical reactions of decomposition products are involved [83,69,75]. Similarly, we could affirm that this phosphate scavenging process is affected by both physical and chemical effects of cavitation. Lastly to definitively exclude a role of the ionic strength or the high conductivity of these solutions we performed further test using concentrated solutions of NaCl,

K_2SO_4 and Na_2SO_4 in which no meaningful enhance of ROS production have been measured or detectable conductivity and redox potential variation. In case of PST the decrease of redox potential is due to formation of reducing species as a consequence of its thermal degradation.

Conclusions

In this work we have described a series of acoustic cavitation-induced effects in homogeneous aqueous solutions of piezo/ferroelectric salts. Although a theory that correlates the chemical effects and plasma formation in cavitation to electrical discharge phenomena has been proposed in the past [84,85,86,87], and the formation of ordered structures has been observed in concentrated solutions of these salts [88,89,90], our unexpected results highlight the absence of a role of piezo/ferroelectric properties in these experiments.

We can state that collapsing bubbles act as transient microreactors that activate the thermal decomposition of salts molecules in concentrated solutions of tartrates, nitrates, and acidic phosphates, and in turn their decomposition products enhance the water sonolysis reactions.

Our experiments have revealed that two different scavenging regions are present: a) within collapsing bubbles and b) at liquid-gas interface. Both regions can be exploited for generating ROS, especially at high frequency, or for H₂ specific generation.. Furthermore, this fundamental study opens a plenty of room to play and tune manifold parameters, deserving future investigations, such as the optimal ultrasonic frequency to activate specific process, the salt types, the salt concentration (i.e. supersaturated solutions), or synergistic effects with piezocatalytic micro/nanoparticles. These results represent a novel starting concept for an optimised use of ultrasonic cavitation, with possibility to control and increase the yield of sonochemical processes in homogeneous aqueous media. With potential application in energy and environmental applications.

Materials and methods

Ultrasonic equipment

Ultrasonic treatments at 20 kHz have been performed using a HD2200 Badelin sonotrode equipped with TT 13 tip dipped 1, 1.5 cm into the solutions, working at 45% of maximum power, corresponding to a power density 5 W/cm^2 as reported from our previous calorimetric measurements [91,92]. High frequency ultrasonic treatments were performed using a Meinhardt high frequency ultrasonic transducer driven by a function generator (Agilent 33250A) and Meinhardt amplifier at 858 kHz with an acoustic pressure of 1.5 MPa measured using calibrated Müller Platte Needle hydrophone (mod 100-100-1). Double jacket water chilled reactors have been used for all the experiments which allow to maintain a temperature of 25 °C (see experimental set-up in S.I. Figure 1 and 2). Time of ultrasonic treatments varies from 10, 20, 40,60,90 min of sonication, depending on the relative measurements to be carried out.

Salts solutions for dyes degradation ROS analysis

Deionized MilliQ water have been used to prepare the solutions. All salts have been purchased from Merck. Salts concentration ranging from 10% up to 30% in weight depending on salt solubility. 0,025 mM solution Methylene Blue, 0,030 mM Methyl Orange and 0.033 mM of Bromo phenol Blue have been tested for dyes degradation

experiments. 30 ppm solution of terephthalic acid (TA) have been used for yield measurements of OH radical through photoluminescence (PL) measurements.

Instrumental equipment

PL has been performed using similar apparatus of figure S1 in SI for 20 kHz while a modified set up (figure S3) have been used for PL measurements at high frequency.

An HORIBA Gemini 180 fluorimeter equipped with double grating scanning monochromator and Xe light source working in excitation mode (310 nm as excitation wavelength) has been used and collection within the range of TA-OH emission has been performed. Several spectra have been collected for each samples using quartz cell and relative uncertainty on total area variation was less than 2%.

μ -GC measurement for gaseous products analyses have been performed using two sealed ultrasonic set-up (see figure S4 and S5 of S.I. for details). Briefly, two sealed reactors (50 ml for low frequency, and 200 ml for high frequency), were connected through two 1/8 vacuum tubes to the μ -GC. Argon (Ar) has been used as a gas carrier flow, and sampling of gas production has been carried out every 5 min during continuous sonication for 20 min. The temperature of the solutions does not exceed 40 °C. Gas sampling has been performed through a Varian 490 micro-GC

equipped with a Molsieve column, after purging of the cell with a continuous Ar flow for 1 h. An Argon flow rate of $25 \text{ ml} \cdot \text{min}^{-1}$ was used to carry the evolved gas (H_2 and CO in our case) from the reactor to the μ -GC.

UV-Vis measurements have been carried out by means of ThermoScientific GENESYS 50 UV using plastic and quartz cell. Each sample have been analysed immediately after sonication using water or pure salts solutions as blank reference. The % of degradation have been calculated by subtraction of total area of the absorbing peak for each dyes tested. Quartz and plastic cuvette have been used depending on different measurment.

Multibubble sonoluminesce (MBSL) spectra were acquired using a set-up similar to one reported in the literature [93]. Briefly, a Titanium (3 mm of diameter) exponential probe (Bandelin MS73) was dipped into a quartz flask filled with 100 ml of different liquids saturated with Argon. MBSL was generated with pulsed ultrasound (25% of maximum power). Light was collected from the bottom with a multicore optical fibers couples to a monochromator (Acton) and analysed with LN cooled CCD camera (Princeton Instruments) Resolution of UV-visible spectra is $1 \pm \text{nm}$, time of acquisition 120 s.

Potential redox of the solution have been measured by means of HQ40 Hach Lange multi-meter equipped with MTC301 potential measurement probe. In case of 30% PST solution the potential decrease form +180 mV to +90 mV after 45 min of sonication at 20 kHz.

The generation of OH radical was investigated using electron spin resonance (EPR) spectroscopy EMXNano X-Band spectrometer (Bruker equipped with Bruker Xenon software) associated with the spin trapping technique which itself used DMPO (5,5-dimethyl-1-pyrroline-N-oxide, Alexis Biochemicals, USA) as spin-probing agent for oxygen radicals. As an example the decrease of EPR signal at 858 kHz in presence of ADP conc 3 % with respect to water is shown in Figure S6 of S.I.

Data availability: The data that support the findings of this study are available from the corresponding author (a.troia@inrim.it) upon reasonable request

Competing Interests statement : The authors declare no competing interests.

Author contributions

A. Troia conceived the study, performed the experiments and formulated hypothesis and conclusion of the work.

V.Cauda and **V. Vighetto** supported the experiments (EPR) and theoretical evaluation.

S. Hernandez and **M. Gallone** support the experiments (GC) and statistical analysis

V. Maurino and **F. Pellegrino** contributed to theoretical model of radical reactions and for the analysis of the measurements.

All authors discussed the results and contributed to the final manuscript

List of captions

Figure 1 Increase of hydrogen production from ultrasonic thermal decomposition of PST solution: (A) UV-vis measurements of Resazurin reduction after sonication at 20 kHz in a 30% PST solution. Black curve: Oxidized form of Resazurin before treatment, green curve: reduced form after treatment. (B) GC measurement of H₂ evolution generated from a 30% solution of PST treated at 20 kHz (black line) and 858 kHz (blue line) respect to water. (C) CO evolution, at 20 kHz and 858 kHz (red lines) respect to hydrogen (black lines) in a 30% solution of PST.

Figure 2 Increase of oxidizing species from ultrasonic thermal decomposition of nitrates solutions: (A) Uv-vis absorption spectra of KI 0.1 M- starch solutions treated at 20 kHz for 15 min (black line) and in presence of KNO₃ (20% in weight, red line). Photo in the inset shows the different colour of KI solutions after US treatment with KNO₃ (right cuvette) or KI solution alone (left). (B) Uv-vis absorption spectra of same solutions treated at 858 kHz for 15 min, photo in the inset shows the different colour in presence of KNO₃ (right cuvette) or KI alone. (C) Uv-vis absorption spectra of KI 0.1M starch solution treated at 20kHz in presence of NaNO₃ (30% in weight, red line) compared to pure KI solutions

Figure 3 Sonochemical degradation of Methylene Blue in acidic phosphates solutions respect to water and ZnO nanoparticles: (A) Degradation of MB solutions at 20 kHz as function of sonication time in 20% aqueous solution of KDP, ADP and NaDP with respect to water. (B) MB degradation efficiency as function of different salts concentrations for an ultrasonic treatment of 20 minutes at 20kHz. (C) Uv-vis spectra for MB degradation at 20 kHz in a solution containing ZnO piezoelectric nanoparticles (0.2% in weight), line, compared to degradation in 20% solution of ADP solution (line). Blue curve is the MB spectrum before the treatment

Figure 4 Sonochemical degradation of Methyl Orange and Bromophenol Blue in acidic phosphates solutions: (A) Degradation of MO solutions at 20 KHz as function of sonication time in 20 % aqueous solution of KDP ADP and with respect to water. (B) Degradation of MO solutions at 858 kHz in presence of ZnO nanoparticles respect pure water and a 30% solution of NaDP (C) Uv-vis spectra of MO degradation in water (green line) and ADP (red line) at 858 kHz for 45 min. (D) UV-vis spectra for Bromophenol blue degradation at 858 kHz for 60 min using 20 % ADP solutions (red line) respect to water (blue line).

Figure 5 Increase of terephthalic acid fluorescence from ROS formation in acidic phosphates solutions exposed to ultrasounds: (A) Photoluminescence spectra (left) of TA solutions treated for 15 min with 20 KHz set-up as function of KDP, ADP and NaDP (conc 10%) with respect to water. (B) Quantified data of several spectra, as function of salts concentration. (C) Photoluminescence spectra (left) of TA solutions treated for 15 min with 858 kHz set-up as function of KDP, ADP and NaDP (conc 10%, also 20% for ADP) with respect to water. (D) Quantified data of several spectra, as function of salts concentration. Temperature of solutions was maintained at 25°C.

Figure 6 Multibubble Sonoluminescence: Sonoluminescence spectra of ADP (red), KDP (violet) and NaDP (orange) solutions compared to water (blue) and H_3PO_4 (black). The region between 300-350 nm shows the different contribution for each solution promoting OH^\bullet and PO^\bullet radical emission band. Emission lines form K, Na atoms and CN group are also well visible.

Acknowledgments

The authors would like to thank Prof. R. Spagnolo for financial support of these experimental investigations and Dott. M. Pelassa for his scientific and technical contribution.

References

1. Suslick, K.S ,Science Volume 247, Issue 4949, Pages 1439 – 14451990
2. E. B. Flint, K. S. Suslick , The temperature of cavitation Science 1991 Sep 20;253(5026):13979.
3. . D. J. Flannigan, K.S. Suslick , Plasma formation and temperature measurement during single bubble cavitation Nature 434, 52–55 (2005)

4. Taylor, K. J. ; Jarman, P. D. The spectra of sonoluminescence Australian Journal of Physics, vol. 23, p.319 June 1970
5. A. A. Ndiaye, R. Pflieger B. Siboulet J. Molina, J.F. Dufrêche, S. I. Nikitenko, Nonequilibrium Vibrational Excitation of OH Radicals Generated During Multibubble Cavitation in Water *+ Vol 116/Issue 20 2012
6. P.Riesz, K. Takashi, Free radical formation induced by ultrasound and its biological implications Free Radical Biology and Medicine Volume 13, Issue 3, Pages 247 -270 September 1992
7. Ohl, C.-D., Kurz, T., Geisler, R., Lindau, O., Lauterborn, W. Bubble dynamics, shock waves and sonoluminescence Philosophical Transactions of the Royal Society A: Mathematical, Physical and Engineering Sciences, 1999, 357(1751), pp. 269–294
8. K. S. Suslick, and G. J. Price Applications Of Ultrasound To Materials Chemistry Annual Review of Materials Research Volume 29, 1999 Review Article
9. T. J. Mason Sonochemistry and the environment – Providing a “green” link between chemistry, physics and engineering Ultrasonics Sonochemistry Volume 14, Issue 4, April 2007, Pages 476-483
10. R. J. Wood, J. Lee, M. J. Bussemaker A parametric review of sonochemistry: Control and augmentation of sonochemical activity in aqueous solutions Ultrasonics Sonochemistry Volume 38, 2017, Pages 351-370
11. . M. Singla, N. Sit Energy Aspects of Acoustic Cavitation and Sonochemistry Fundamentals and Engineering 2022, Pages 349-373 Chapter 21 - Raising challenges of ultrasound-assisted processes and sonochemistry in industrial applications based on energy efficiency, Book Chapter ISBN 978-032391937-1, 978-032398490-4 DOI 10.1016/B978-0-323-91937-1.00017-7
12. Y. Asakura, K. Yasuda Frequency and power dependence of the sonochemical reaction Ultrasonics Sonochemistry 81 (2021) 105858
13. C. Murali Krishna, P.Riesz, K. Takashi Free radical formation by ultrasound in aqueous solutions. A spin trapping study Free Radical Research Volume 10, Issue 1-2, Pages 27 – 35 1990
14. M. Sharifishourabi, I. Dincer, A. Mohany Implementation of experimental techniques in ultrasound-driven hydrogen production: A comprehensive review International Journal of Hydrogen Energy 62 (2024) 1183–1204
15. Henglein, A. & Kormann, C. Scavenging of OH radicals produced in the sonolysis of water. Int. J. Radiation Biol. Related Stud. Phys. Chem. Med. 48, 251–258 (1985).

16. H. E. Hansen, F. Seland, S. Sunde, O.S. Burheim & B. G. Pollet Optimum scavenger concentrations for sonochemical nanoparticle synthesis *Scientific Reports* | (2023) 13:6183
17. Buettner, J., Gutierrez, M. & Henglein, A. Sonolysis of water-methanol mixtures. *J. Phys. Chem.* 95, 1528–1530 (1991).
18. Kohno, T. Mokudai, T. Ozawa, Y. Niwano Free radical formation from sonolysis of water in the presence of different gases Masahiro 1,* *J Clin Biochem Nutr* . 2011 ;49(2):96–101
19. B. Gielen, S. Marchal, J. Jordens, L.C.J. Thomassen, L. Braeken, T. Van Gerven Influence of dissolved gases on sonochemistry and Sonoluminescence in a flow reactor *Ultrasonics Sonochemistry* 31 (2016) 463–472
20. K.-Sheng Hong, H. Xu, H. Konishi, and X. Li, Direct Water Splitting Through Vibrating Piezoelectric Microfibers in Water *J. Phys. Chem. Lett.* 2010, 1, 997–1002
21. K.-Sheng Hong, H. Xu, H. Konishi,† and X. Li Piezoelectrochemical Effect: A New Mechanism for Azo Dye Decolorization in Aqueous Solution through Vibrating Piezoelectric Microfibers *J. Phys. Chem. C* 2012, 116, 13045–13051
22. M. Ahmad E. Ahmed, Z.L. Hong, W. Ahmed, A. Elhissi, N.R. Khalid; Photocatalytic, sonocatalytic and sonophotocatalytic degradation of Rhodamine B using ZnO/CNTs composites photocatalysts *Ultrasonics Sonochemistry* 21 (2014) 761–773
23. V. Morosini, T.Chave, M. Viro, P. Moisy, S. I. Nikitenko Sonochemical water splitting in the presence of powdered metal oxides *Ultrasonics Sonochemistry* 29 (2016) 512–516
24. Z. Lianga, C. Feng Yana, S. Rtimib, J. Bandarac ;Piezoelectric materials for catalytic/photocatalytic removal of pollutants: Recent advances and outlook *Applied Catalysis B: Environmental* 241 (2019) 256–269
25. F. Bösl, T.P. Comyn, P. I. Cowin, F. R. García-García, I. Tudela, ; Piezocatalytic degradation of pollutants in water: Importance of catalyst size, poling and excitation mode *Chemical Engineering Journal Advances* 7 (2021) 100133
26. H. You, Z. Wu,* L. Zhang, Y. Ying, Y. Liu, L. Fei, X. Chen, Y. Jia, Y. Wang, F. Wang, S. Ju, J. Q. Chi-Hang Lam, and H. Huang Harvesting the Vibration Energy of BiFeO₃ Nanosheets for Hydrogen Evolution *Angew Chem Int Ed Engl* . 2019 Aug 19;58(34):11779-11784.
27. Y. Wang, Y. Xu, S. Dong, P. Wang, W. Chen, Z. Lu, D. Ye, B. Pan, DiWu, C. D. Vecitis & G. Gao;Ultrasonic activation of inert poly (tetrafluoroethylene) enables piezocatalytic generation of reactive oxygen species *Nat Commun* . 2021 Jun 9;12(1):3508. doi: 10.1038/s41467-021-239213.

28. P. Thi, T. Phuong, Y. Zhang, N., G. Hamideh, N. Phuc, H. Duy, X. Zhou, D. Zhang, K. Zhou, S. Dunn and C. Bowen, Demonstration of Enhanced Piezo-Catalysis for Hydrogen Generation and Water Treatment at the Ferroelectric Curie Temperature *iScience* 23, 101095, 2020 .
29. G. Nie, Y. Yao, X. Duan, L. Xiao and S. Wang; Advances of piezoelectric nanomaterials for applications in advanced oxidation technologies *Current Opinion in Chemical Engineering* 2021, 33:100693
30. W. Qian, W. Yang, Y. Zhang, C. R. Bowen, Y. Yang ; Piezoelectric Materials for Controlling Electro-Chemical Processes *Nano-Micro Lett.* (2020) 12:149
31. S. Li, Z. Zhao, J. Li, H. Liu, M. Liu, Y. Zhang, L. Su, A. Isabel Pérez-Jiménez, Y. Guo, F. Yang, Y. Liu, J. Zhao, J. Zhang, Li-Dong Zhao, and Y. Lin; Mechanically Induced Highly Efficient Hydrogen Evolution from Water over Piezoelectric SnSe nanosheets *Small* 2022, 18, 2202507
32. C. Wang, C. Hu, F. Chen, T. Ma, Y. Zhang, H. Huang ; Design strategies and effect comparisons toward efficient piezocatalytic system *Nano Energy* Volume 107, March 2023, 108093
33. K. Wang, C. Han, J. Li, J. Qiu, J. Sunarso and S. Liu ; The Mechanism of Piezocatalysis: Energy Band Theory or Screening Charge Effect? *Angew. Chem. Int. Ed.* 2022, 61, e202110429
34. Y. Zhang, H. Khanbareh, S. Dunn, C. Bowen, H. Gong, N. Phuc H. Duy, and P. Thi T. Phuong; High Efficiency Water Splitting using Ultrasound Coupled to a BaTiO₃ Nanofluid *Adv. Sci.* 2022, 9, 210524
35. Bößl, F., Menzel, V.C., Chatzisyseon, E., I. Tudela, I. Effect of frequency and power on the piezocatalytic and sonochemical degradation of dyes in water *Chemical Engineering Journal Advances*, 2023, 14, 100477
36. F. Bößl and I. Tudela ; Piezocatalysis: Can catalysts really dance? *Current Opinion in Green and Sustainable Chemistry* 2021, 32:100537
37. Y. Jiang, J. Liang, F. Zhuo, H. Ma, S. S. Mofarah, C. C. Sorrell, D. Wang, and P. Koshy Unveiling Mechanically Driven Catalytic Processes: Beyond Piezocatalysis to Synergetic Effects <https://doi.org/10.1021/acsnano.5c02660> Published May 6, 2025
38. Y. Jiang, J. Liang, F. Zhuo, H. Ma, S. S. Mofarah, C. C. Sorrell, D. Wang, and P. Koshy* Unveiling Mechanically Driven Catalytic Processes: Beyond Piezocatalysis to Synergetic Effects <https://doi.org/10.1021/acsnano.5c02660> Published May 6, 2025

39. R. Mohanty, S. Mansingh, K. Parida, Boosting sluggish photocatalytic hydrogen evolution through piezo-stimulated polarization: a critical review *Mater. Horiz.*, 2022, 9, 1332–1355 | 1333
40. L. Jing , Y. Xu , M. Xie, Z. Li, C. Wu, H. Zhao , J. Wang , H. Wang, Y. Yan, N. Zhong H. Li, J. Hu a Piezo-photocatalysts in the field of energy and environment: Designs, applications, and prospects *Nano Energy* Volume 112, July 2023, 108508
41. H. Dong , Y. Zhou , L. Wang , L.Chen , M. Zhu Oxygen vacancies in piezocatalysis: A critical review *Chemical Engineering Journal* Volume 487, 1 May 2024, 150480
42. N. Domingo Understanding piezocatalysis, pyrocatalysis and ferrocatalysis *Front. Nanotechnol.* 6:1320503
43. I. Hossain and G. J. Blanchard Ionic Liquids Exhibit the Piezoelectric Effect *Md. J. Phys. Chem. Lett.* 2023, 14, 2731–2735
44. W. P. Mason Piezoelectricity, its history and applications *J. Acoust. Soc. Am.* 70, 1561–1566 (1981)
45. T. Nagamiya On the Theory of the Dielectric, Piezoelectric, and Elastic Properties of $\text{NH}_4\text{H}_2\text{PO}_4$ *Progress of Theoretical Physics*, Volume 7, Issue 3, March 1952, Pages 275–284
46. Scott, J.F., Duiker, H.M., Beale, P.D. Butler, D., Eaton, S.; Properties of ceramic KNO_3 thin-film memories *Physica B+C*, 1988, 150(1-2), pp. 160–167
47. Samara, G.A.;The effects of deuteration on the static ferroelectric properties of KH_2PO_4 (kdp) *Ferroelectrics*, 1973, 5(1), pp. 25–37
48. S. Koda, T. Kimura, T. Kondo, H. Mitome, A standard method to calibrate sonochemical efficiency of an individual reaction system *Ultrasonics Sonochemistry* ,10, 3, 2003, Pages 149-156
49. D. Bhai Rajamma , S. Anandan, N. Saadah, M. Yusof, B. G. Pollet, M. Ashokkumar; Sonochemical dosimetry: A comparative study of Weissler, Fricke and terephthalic acid methods, *Ultrasonics Sonochemistry* 72 (2021) 105413
50. Y.Nan Liu, X. Zhou, X. Wang, K. Liang, Z.-Kun Yang, C.-Cong Shen, M. Imran, S. Sahar and A.Wu Xu ; Hydrogenation/oxidation induced efficient reversible color switching between methylene blue and leuco-methylene blue *RSC Adv.*, 2017, 7, 30080
51. Zalata, A., Hafez, T., Mahmoud, A., Comhaire, F.Andrology: Relationship between resazurin reduction test, reactive oxygen species generation, and γ -glutamyltransferase *Human Reproduction*, 1995, 10(5), pp. 1136–1140

52. N. Merabet , K. Kerboua ; Sonolytic and ultrasound-assisted techniques for hydrogen production: A review based on the role of ultrasound *International Journal of Hydrogen Energy* 47 (2022) 17879 e17893
53. R. Ma, H. Su, J. Sun, D. Li, Z. Zhang, J. Wei; Thermally-enhanced sono-photo-catalysis by defect and facet modulation of Pt-TiO₂ catalyst for high-efficient hydrogen evolution, *Ultrasonics Sonochemistry* 90, 2022, 106222
54. M. W. Ruzsyczky and V. E. Anderson* Tartrate dehydrogenase reductive decarboxylation: stereochemical generation of diastereotopically deuterated hydroxymethylenes, *Bioorganic Chemistry* 32 (2004) 51–61
55. V. Mathivanana,*, M. Harisb, J. Chandrasekaran; Thermal, magnetic, dielectric and anti microbial properties of solution-grown pure and doped sodium potassium tartrate crystals *Optik* 127 (2016) 1804–1808
56. Eli S. Freeman The Kinetics of the Thermal Decomposition of Potassium Nitrate and of the Reaction between Potassium Nitrite and Oxygen *J. Am. Chem. Soc.* 1957, 79, 4, 838–842
57. T. Kimura , T. Sakamoto, J.-M. Leveque, H. Sohmiya, M. Fujita, S. Ikeda, T. Ando Standardization of ultrasonic power for sonochemical reaction *Ultrasonics Sonochemistry* Volume 3, Issue 3, November 1996,
58. E. Fraím, A. Serna-Galvis, R. A. Torres-Palma; An experimental class to illustrate the physical and chemical effects of ultrasound as an introduction to practical advanced oxidation processes *Ultrasonics Sonochemistry* 112, 2025
59. S. Koda, T. Kimura, T. Kondo, H. Mitome, A standard method to calibrate sonochemical efficiency of an individual reaction system *Ultrasonics Sonochemistry* ,10, 3, 2003, Pages 149-156
60. S. I Bannov , V. A Nevostruev; Formation and properties of NO₂⁻, NO₃ and ONOO radicals in nitrate-containing matrices *Radiation Physics and Chemistry* Volume 68, 5, 2003, Pages 917- 924
61. D. Bhai Rajamma , S. Anandan, N. Saadah, M. Yusof, B. G. Pollet, Muthupandian Ashokkumar; Sonochemical dosimetry: A comparative study of Weissler, Fricke and terephthalic acid methods, *Ultrasonics Sonochemistry* 72 (2021) 105413
62. Y. Wang, J. Jing Yang, J. He, X. Ping Wen, W. Tao Ji, and Y. Wang Inhibition Effect of KHCO₃ and KH₂PO₄ on Ethylene Explosion *ACS Omega* 2023, 8, 7566–7574
63. H. Jiang, M. Bi, B. Li, D. Ma, W. Gao; Flame inhibition of aluminum dust explosion by NaHCO₃ and NH₄H₂PO₄ , *Combustion and Flame* 200 (2019) 97–114

64. Q. Wang, X. Jiang, J. Deng, Z. Luo, Q. Wang, Z. Shen, C.-Min Shu, B. Peng, C. Yu ; Analysis of the effectiveness of $Mg(OH)_2/NH_4H_2PO_4$ composite dry powder in suppressing methane explosion *Powder Technology* 417 (2023) 118255
65. M. Yu, F. Wang , H. Li, F. Zhai , J. Wang , S. Li ; Macroscopic behaviors and chemical reaction mechanism for the inhibition of $NH_4H_2PO_4$ powder in hybrid methane/coal dust deflagrations *Fuel* 356 (2024) 129558
66. L. Fijołek, J. Nawrocki Phosphate helps to recover from scavenging effect of chloride in selfenhanced ozonation *Chemosphere* 212 (2018) 802-810
67. M. Yu, F. Wang , H. Li , F. Zhai , J. Wang , S. Li Macroscopic behaviors and chemical reaction mechanism for the inhibition of $NH_4H_2PO_4$ powder in hybrid methane/coal dust deflagrations *Fuel* 356 (2024) 129558
68. J. A. Rosso, F. J. Rodriguez Nieto, M. C. Gonzalez , D. O. Matire ' Reactions of phosphate radicals with substituted benzenes *Journal of Photochemistry and Photobiology A: Chemistry* 116 (1998) 21-25
69. T. Vlase, G. Vlase and N. Doca Kinetics Of Thermal Decomposition Of Alkaline Phosphates *Journal of Thermal Analysis and Calorimetry*, Vol. 80 (2005) 207–210
70. Y. Sun, S. Zhu, L. Tao, X. Wu Experimental Study on Suppression of $NH_4H_2PO_4$ on Cassava Starch Dust Explosion Proceedings of the 2023 5th International Conference on Hydraulic, Civil and Construction Engineering (HCCE 2023) Atlantis Highlights in Engineering
71. Q. Wang, Y. Sun, J. Jiang, J. Deng, C. Min Shu, Z. Luo, Q. Wang; Inhibiting effects of gas– particle mixtures containing CO_2 , $Mg(OH)_2$ particles, and $NH_4H_2PO_4$ particles on methane explosion in a 20-L closed vessel *Journal of Loss Prevention in the Process Industries* 64 (2020) 104082
72. O.P. Korobeinichev, V.M. Shvartsberg, A.G. Shmakov, D.A. Knyazkov, I.V. Rybitskaya Inhibition of atmospheric lean and rich $CH_4/O_2/Ar$ flames by phosphorus-containing Compound Proceedings of the Combustion Institute 31 (2007) 2741–2748
73. Z. Li, W. Zhao, C. Li, Z. Fan, M. Chen, L. Xian The characteristics and mechanism of core-shell structure fly ash/ KH_2PO_4 composite inhibitor in suppressing coal dust explosions *Journal of Loss Prevention in the Process Industries*
74. C. Fei Yu, B. Jiang, L. Yuan, Y. Zhang, B. Ji , Y. Zheng , B. Ren Inhibiting effect investigation of ammonium dihydrogen phosphate on oxidative pyrolysis characteristics of bituminous coal *Fuel* 333 (2023) 126352

75. T.M. Jayaweera , C.F. Melius , W.J. Pitz , C.K. Westbrook, O.P. Korobeinichev , V.M. Shvartsberg, A.G. Shmakov, I.V. Rybitskaya, H.J. Curran Flame inhibition by phosphorus- containing compounds over a range of equivalence ratios , *Combustion and Flame* 140 (2005) 103–115
76. H. Xu, N. G. Glumac, and K. S. Suslick , Temperature Inhomogeneity during Multibubble Sonoluminescence** *Angew. Chem. Int. Ed.* 2010, 49, 1079 –1082
77. D. Wang, Q., W. Bao, H. Han, and Naranmandula; Dancing bubble sonoluminescence in phosphoric acid solution, *Chin. Phys. B* 33, 117803 (2024)
78. A. Aghelmaleki, H. A. C. Cairós, R. Pflieger, R Mettin; Effect of mechanical stirring on sonoluminescence and sonochemiluminescence *Ultrasonics Sonochemistry*, 111, 2024, 107145
79. K. Peng, S. Tian, Y Zhang, Q. He, Q. Wang Penetration of hydroxyl radicals in the aqueous phase surrounding a cavitation bubble *Ultrasonics Sonochemistry*, 91, 106235 *Ultrasonics Sonochemistry* Volume 91, December 2022, 106235
80. Cairós, C., Schneider, J., Pflieger, R., Mettin, R. Effects of argon sparging rate, ultrasonic power, and frequency on multibubble sonoluminescence spectra and bubble dynamics in NaCl aqueous solutions *Ultrasonics Sonochemistry*, 2014, 21(6), pp. 2044–2051
81. S.I. Nikitenko, L. Venault Ph. Moisy Scavenging of OH radicals produced from H₂O sonolysis with nitrate ions *Ultrasonics Sonochemistry* 11 (2004) 139–142
82. E. Dalodière , M. Viroto , P. Moisy , S. I. Nikitenko Effect of ultrasonic frequency on H₂O₂ sonochemical formation rate in aqueous nitric acid solutions in the presence of oxygen *Ultrasonics Sonochemistry* 29 (2016) 198–204
83. A Pardo, J Romero and E Ortiz; High-temperature behaviour of ammonium dihydrogen phosphate *IOP Conf. Series: Journal of Physics: Conf. Series* 935 (2017) 012050
84. M.A. Margulis*, I.M. Margulis Theory of local electrification of cavitation bubbles: new approaches *Ultrasonics Sonochemistry* 6 (1999) 15–20
85. M. A. Margulis The Kinetic Equations of the Electron-Diffusion Model of the Space–Time Distribution of Radicals in a Cavitation Field *Russian Journal of Physical Chemistry A*, 2008, Vol. 82, No. 8, pp. 1407–1411
86. M. A. Margulis and I. M. Margulis Current State of the Theory of Local Electrification of Cavitation Bubbles *Russian Journal of Physical Chemistry A*, 2007, Vol. 81, No. 1, pp. 129– 138
87. V Pilgunov 1 and K Efremova Electro-hydronechanical processes in mineral oil flow *IOP Conf. Series: Materials Science and Engineering* 779 (2020) 012032

88. M. K. Cerreta And K. A. Berglund ; The Structure Of Aqueous Solutions Of Samedihydrogen Orthophosphates By Laser Raman Spectroscopy *Journal of Crystal Growth* 84 (1987) 577–588
89. C. Sun, D. Xue ; Hydrogen bonding nature during ADP crystallization *Journal of Molecular Structure* 1059 (2014) 338–342
90. H. V. Alexandru Second-order transition in Rochelle-salt saturated solutions *Physical Review A* Volume 45, Number 12 15 June 1992
91. A. Troia a, S. Galati a, V. Vighetto b, V. Cauda b Piezo/sono-catalytic activity of ZnO micro/nanoparticles for ROS generation as function of ultrasound frequencies and dissolved gases *Ultrasonics Sonochemistry* 97 (2023) 106470
92. A. Troia, E.S. Olivetti, L. Martino, V. Basso Sonochemical hydrogenation of metallic microparticles, *Ultrasonics - Sonochemistry* 55 (2019) 1–7
93. A. Troia , D. Madonna Ripa The role of vapour pressure in multibubble sonoluminescence from organic solvents , *Ultrasonics Sonochemistry* 18 (2011) 1180–1184

Table 1 Thermal and ultrasonic ())) reactions of water radicals and acidic phosphates radicals

RADICAL REACTIONS	APPLICATION OR STUDY	Ref
$\text{H}_2\text{O} \rightarrow \text{OH}\cdot + \text{H}\cdot$	1 ultrasound water sonolysis	4,5
$2\text{OH}\cdot \rightarrow \text{H}_2\text{O}_2$	2 radical recombination reaction	4,5
$\text{NH}_4\text{H}_2\text{PO}_4 \rightarrow \text{NH}_3 + \text{H}_3\text{PO}_4$	3 Thermal degradation of ADP	59,61
$\text{NH}_3 + \text{OH}\cdot \rightarrow \text{NH}_2 + \text{H}_2\text{O}$	4 Gas phase reaction of flame suppression for ADP	59,61
$\text{H}_3\text{PO}_4 \rightarrow \text{HOPO}_2 + \text{H}_2\text{O}$	5 Policondesation and degradation of phosphate in flame suppression	58,57
$\text{KH}_2\text{PO}_4 \rightarrow \text{KPO}_3 + \text{H}_2\text{O}$	6 Thermal degradation of KDP in flame suppression	63,67
$\text{H}_2\text{PO}_4^- + \text{OH}\cdot \rightarrow \text{HPO}_4^{\cdot-} + \text{H}_2\text{O}$	7 Radical reaction of phosphate in self-enhanced ozonation process	60
$\text{HPO}_4^{\cdot-} + \text{H}^+ \rightarrow \text{H}_2\text{PO}_4\cdot$	8 Radical reaction of phosphate in self-enhanced ozonation process	60
$\text{H}_2\text{PO}_4\cdot + \text{H}_2\text{O}_2 \rightarrow \text{H}^+ + \text{HO}_2\cdot + \text{H}_2\text{PO}_4^-$	9 Flash photolysis study on degradation Of Nitrobenzene by phosphate	62,64
$\text{HOPO}_2 \rightarrow \text{PO}\cdot + \text{HO}_2\cdot$	10 Radical reaction of HOPO ₂ in flame suppression	61,69

$\text{PO}\cdot + \text{H}\cdot \rightarrow \text{HPO}\cdot$	11	Radical scavenging reaction	67,68
$\text{HOPO}_2\cdot + \text{H}\cdot \rightarrow \text{PO}_2 + \text{H}_2\text{O}$	12	Radical reaction of HOPO ₂ radical in flame suppression	66,65,68
$\text{HOPO}_2\cdot \rightarrow \text{PO}_2 + \text{OH}\cdot$	13	Radical reaction of HOPO ₂ radical in flame suppression	59,69
$\text{PO}_2 + \text{H}\cdot \rightarrow \text{HOPO}\cdot$	14	Scavenging reaction of H· radical in flame suppression	66,68
$\text{HOPO}\cdot + \text{OH}\cdot \rightarrow \text{PO}_2 + \text{H}_2\text{O}$	15	Termination reaction of flame suppression	58,69

Editor summary:

Enhancing the yield of radical reactions generated by ultrasonic cavitation in aqueous media has historically focused on the role of volatile or surfactant molecules entering within the bubbles to scavenge aqueous radicals. Here, the authors report an unexpected scavenging mechanism activated by thermal degradation of salts exposed to the transient hot temperatures generated by ultrasound in homogeneous solutions, with an effect on radical selectivity as function of the salts tested leading to an increase of reactive oxygen species or H₂ gas, or to the formation of oxidizing species, revealing a new approach for modulating sonochemical reactions in aqueous solutions.

Peer review information:

Communications Chemistry thanks Timothy Mason and the other, anonymous, reviewer(s) for their contribution to the peer review of this work. A peer review file is available.

Graphical Abstract

